Molecular and structural basis of pan-resistance to BTK targeting therapies via BTK A428D mutation

Q. Sievers[1], H. Lu[2], A. Cool[3], S. Gajewski[2], T. Kong[1], M. Noviski[2], E. Ficici[2], R. Mukerji[2], J. Iuliano[2], J. Ye[2], M. Sanchez Garcia de los Rios[2], H. Bousquet[2], S. Whelan[2], M. Tan[2], C. Phelps[2], X. Mi[1], J. Rahman[1], L. Mendoza Navarrete[1], S. Sekeres[3], E. Lamkin[3], E. Bravo[3], M. Ewalt[1], A. Mato[4], L. Roeker[5], J. Taylor[3], M. Thompson[1], G. Hansen[2], O. Abdel-Wahab[1]

Memorial Sloan Kettering Cancer Center

NURIX

INTRODUCTION

BTK degraders (BTKd) are bifunctional small molecules that mediate the interaction of BTK with the cereblon E3 ubiquitin ligase, thereby resulting in BTK's ubiquitination and proteasomal degradation.

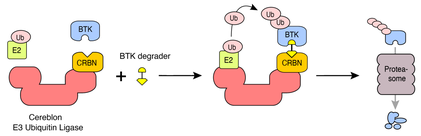

In clinical studies BTK degraders have achieved responses in B cell malignancies with mutations in BTK that confer resistance to conventional BTK inhibitors (BTKi).

RATIONALE

How the unique selection pressure of BTK degraders will shape clinical mechanisms of resistance is unknown.

Understanding these mechanisms will inform 1) treatment sequencing and combination regimens, 2) the development of next-generation BTK degraders and, 3) the broader field of targeted protein degradation therapeutics.

APPROACH

1. Sequence pre- and post-treatment patient samples from the phase 1 trial of the first-in-class BTK degrader, zelebrudomide (NX-2127), using MSK-IMPACT heme, a 500 gene hybrid-capture exome sequencing panel with VAF cutoff of >2%.
2. Characterize mutations in the BTK-dependent DLBCL cell line, TMD8, using cellular, molecular, biochemical, and structural assays.

Affiliations

1. Memorial Sloan Kettering, New York, NY, United States
2. Nurix Therapeutics, Brisbane, CA, United States
3. University of Miami, Miami, FL, United States
4. Cayuga Health, Ithaca, NY, United States
5. Mayo Clinic, Rochester, MN, United States

RESULTS

1. BTK A428D is a treatment-emergent mutation observed following zelebrudomide

Four patients with CLL developed progressive disease following treatment with zelebrudomide and exhibited the following mutations newly detectable above 2% VAF in post-treatment samples:

Patient 1. **BTK A428D (Figure 1)**
Patient 2. PLCG2 D993Y, PLCG2 D1140N, CARD11 V726D, PDS5B K1031Q
Patient 3. TP53 V216L
Patient 4. No new mutations

In patient 1, deeper sequencing identified BTK A428D at baseline (# in the graph), showing <2% VAF with strong bidirectional reads, high-quality base calls, and deep coverage.

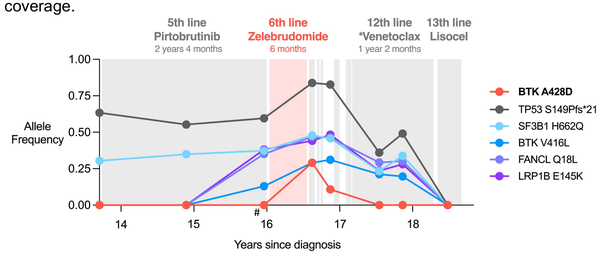

Figure 1 | Mutation frequency in patient 1 before and after treatment with zelebrudomide. *12th line therapy with venetoclax also included obinutuzumab and radiation.

2. BTK A428D is pan-resistant to BTKi and BTKd but, without selection, exhibits a fitness defect

To model clonal competition we mixed TMD8 parental and BTK A428D knock-in cells at a 95:5 ratio and then treated them with 0.1μM BTKi or BTKd for 21 days. Following an initial period of growth suppression a resistant population emerged in each condition (**Figure 2A**). Sequencing revealed expansion of BTK A428D to >90% (**Figure 2B**). However, in the DMSO control the frequency of BTK A428D decreased from 5% to <0.5%, suggesting that the mutation may confer a fitness defect.

To quantify the degree of resistance we also performed CellTiter-Glo viability assays on TMD8 parental and knock-in BTK-mutant cell lines. Unlike the other BTKi resistance mutations tested the A428D mutation conferred near-complete insensitivity to all BTKi and BTKd (**Figure 2C**).

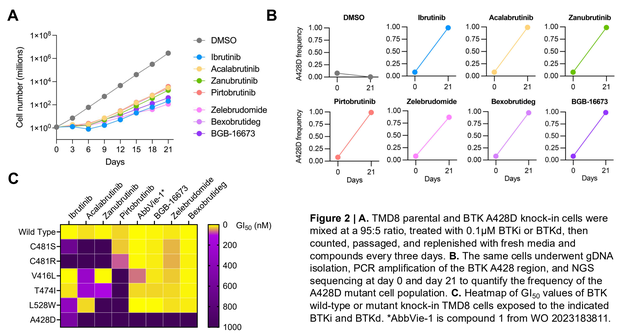

Figure 2 | A. TMD8 parental and BTK A428D knock-in cells were mixed at a 95:5 ratio, treated with 0.1μM BTKi or BTKd, then counted, passaged, and replenished with fresh media and compounds every three days. **B.** The same cells underwent gDNA isolation, PCR amplification of the BTK A428 region, and NGS sequencing at day 0 and day 21 to quantify the frequency of the A428D mutant cell population. **C.** Heatmap of GI_{50} values of BTK wild-type or mutant knock-in TMD8 cells exposed to the indicated BTKi and BTKd. *AbbVie-1 is compound 1 from WO 2023183811.

3. BTK A428D prevents degradation of BTK

To determine if drug resistance was due to a lack of BTK degradation we treated TMD8 parental and BTK A428D knock-in cells with clinical stage BTKd for 24 hours and assessed endogenous BTK levels via western blot. Indeed, BTK A428D prevented BTKd-induced degradation (**Figure 3A**).

We confirmed this using an orthogonal assay in TMD8 cells that were lentivirally transduced with a BTK-eGFP degradation reporter. Cells were treated with a titration of BTKd for 20 hours and degradation was assessed via flow cytometry (**Figure 3B**). Again, BTK A428D exhibited near-complete insensitivity.

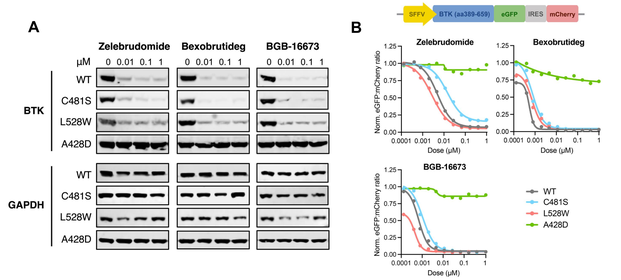

Figure 3 | A. TMD8 parental and BTK A428D knock-in cells were treated with BTKd for 24 hours followed by lysis and western blotting for BTK. **B.** Parental TMD8 cells were lentivirally transduced with a BTK-eGFP degradation reporter, treated with a titration of zelebrudomide, bexobrutideg, or BGB-16673 for 20 hours, and then reporter degradation was assessed via flow cytometry (eGFP:mCherry ratio normalized to DMSO condition).

4. BTK A428D resists binding by BTKi, BTKd, and broad-spectrum kinase tracers

To assess if BTK A428D prevented the BTKd-induced interaction of BTK and cereblon we performed a NanoBRET ternary complex assay in HEK293T cells. BTK A428D completely blocked ternary complex formation (**Figure 4A**).

Next, to determine if BTK A428D prevented BTKi and BTKd from binding, we used SPR to measure small-molecule interaction with full-length recombinant BTK. None of the compounds showed measurable binding (**Figure 4B**).

Intriguingly, a panel of 7 tracers based on broad-spectrum, ATP-competitive kinase binders were also unable to bind to BTK A428D in a NanoBRET assay in HEK293T cells, suggesting that BTK A428D's binding pocket was unusually resistant to small molecule binding (**Figure 4C**).

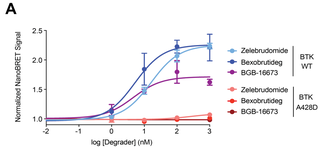

Figure 4 | A. NanoBRET in HEK239T cells measuring BTKd-induced ternary complex formation between BTK and cereblon. **B.** K_D of BTKi and BTKd as determined by SPR. Covalent inhibitors with measurable interaction are reported as "binding". "No binding" indicates no detectable interaction at the top concentration (mean ± SD of 3 or more exp. rep.). **C.** NanoBRET assay with indicated Promega tracers in HEK293T cells.

B

Drug Class	Compound	Full Length, K_D (nM)	
		BTK WT	BTK A428D
Covalent Inhibitor	Ibrutinib	Binding	No binding
	Acalabrutinib	Binding	No binding
	Zanubrutinib	Binding	No binding
Noncovalent Inhibitor	Pirtobrutinib	1.3 ± 0.2	No binding
	Nemtabrutinib	0.74 ± 0.16	No binding
Degrader	AbbVie-1	1.1 ± 0.2	No binding
	BGB-16673	0.69 ± 0.21	No binding
	Zelebrudomide	20 ± 2	No binding
	Bexobrutideg	3.2 ± 0.4	No binding

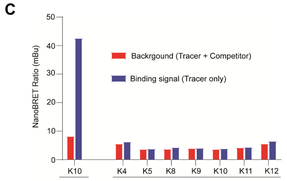

5. Steric clash with mutant aspartate and an auto-inhibited A-loop conformation blocks drug binding

We next solved the crystal structure of apo BTK A428D (aa 382-658) at 1.8Å resolution and found that the mutation prevents drug binding through two mechanisms: First, the aspartate sidechain is shifted into the C-spine cavity where it would obstruct substrates and small molecules that interact with the hinge region of the kinase (**Figure 5A**).

Second, while a portion of the A-loop helix was disordered in our crystal structure, the positioning of the start of the A loop along with the overall similarity to an autoinhibited form of BTK previously observed in a BTK-branebrutinib bound structure suggests that in this conformation the entire A loop extends into the substrate binding pocket where it is predicted to clash with ligands accessing the back and H3 pockets (**Figure 5B**).

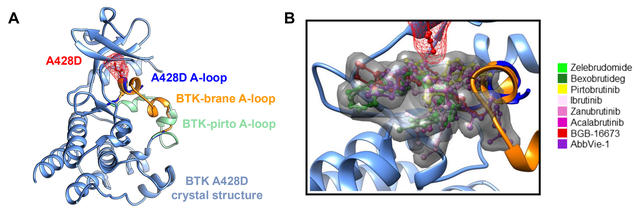

Figure 5 | A. BTK A428D crystal structure (blue) with the position of A-loop (dark blue) and overlap with autoinhibited A-loop conformation (orange; BTK-branebrutinib) and the contrasting A-loop location in BTK-pirtobrutinib (pale-green). **B**. Same figure now with representative structures of BTKi and BTKd bound to BTK, illustrating the clashes both with the mutant aspartate as well as the autoinhibited A-loop conformation.

6. Combination therapy with venetoclax mitigates the outgrowth of BTK A428D tumors

To determine if combining zelebrudomide with a second agent would mitigate the expansion of BTK A428D we introduced a 1:1 mixture of TMD8 parental and BTK A428D knock-in cells via subcutaneous flank injection into NSG mice then treated them with venetoclax (100 mg/kg), zelebrudomide (10 mg/kg or 30 mg/kg), BGB-16673 (20 mg/kg), or zelebrudomide + venetoclax (**Figure 6A**). The combination of zelebrudomide and venetoclax controlled tumor growth better than either agent alone (**Figure 6B**).

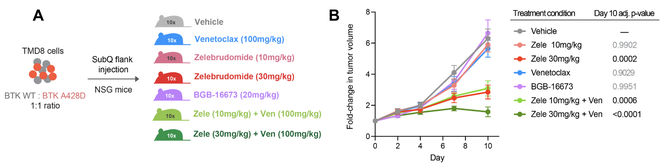

Figure 6 | A. Experimental schematic. TMD8 parental and BTK A428D knock-in cells were mixed at a 1:1 ratio and injected subcutaneously into flanks of NSG mice. After reaching an average tumor volume of >200mm^3 mice were treated daily with indicated compounds. **B.** Fold-change in tumor volume over time. N=10 mice/group. Tumors measured on day 9 or day 10 plotted together on day 10. Mean±SEM shown. P-value for day 10 is one-way ANOVA with Dunnett's correction.

CONCLUSIONS

1. BTK A428D is a treatment-emergent resistance mutation that confers pan-resistance to both BTK inhibitors and degraders.
2. BTK A428D prevents access to the ligand-binding pocket through steric clash induced by the mutant aspartate and stabilization of the A-loop in an autoinhibited conformation.
3. Combination strategies, such as pairing BTKd with other therapies may mitigate expansion of the A428D pan-resistant clone.